



# Size distribution and source of black carbon aerosol in urban Beijing during winter haze episodes

Yunfei Wu<sup>1</sup>, Xiaojia Wang<sup>1</sup>, Jun Tao<sup>2</sup>, Rujin Huang<sup>3</sup>, Ping Tian<sup>4</sup>, Junji Cao<sup>3</sup>, Leiming Zhang<sup>5</sup>, Kin-Fai Ho<sup>6</sup>, Zhiwei Han<sup>1</sup>, and Renjian Zhang<sup>1</sup>

<sup>1</sup>CAS Key Laboratory of Regional Climate-Environment for Temperate East Asia, Institute of Atmospheric Physics, Chinese Academy of Sciences, Beijing, China

<sup>2</sup>South China Institute of Environmental Sciences, Ministry of Environmental Protection, Guangzhou, China

<sup>3</sup>CAS Key Laboratory of Aerosol Chemistry and Physics, Institute of Earth Environment, Chinese Academy of Sciences, Xi'an, China

<sup>4</sup>Beijing Weather Modification Office, Beijing, China

<sup>5</sup>Air Quality Research Division, Science and Technology Branch, Environment and Climate Change Canada, Toronto, Canada

<sup>6</sup>The Jockey Club School of Public Health and Primary Care, The Chinese University of Hong Kong, Hong Kong, China

Correspondence to: Yunfei Wu (wuyf@mail.iap.ac.cn) and Renjian Zhang (zrj@mail.iap.ac.cn)

Received: 5 December 2016 – Discussion started: 6 December 2016

Revised: 1 June 2017 – Accepted: 4 June 2017 – Published: 30 June 2017

**Abstract.** Black carbon (BC) has important impact on climate and environment due to its light absorption ability, which greatly depends on its physicochemical properties including morphology, size and mixing state. The size distribution of the refractory BC (rBC) was investigated in urban Beijing in the late winter of 2014, during which there were frequent haze events, through analysis of measurements obtained using a single-particle soot photometer (SP2). By assuming void-free rBC with a density of  $1.8 \text{ g cm}^{-3}$ , the mass of the rBC showed an approximately lognormal distribution as a function of the volume-equivalent diameter (VED), with a peak diameter of 213 nm. Larger VED values of the rBC were observed during polluted periods than on clean days, implying an alteration in the rBC sources, as the size distribution of the rBC from a certain source was relative stable, and VED of an individual rBC varied little once it was emitted into the atmosphere. The potential source contribution function analysis showed that air masses from the south to east of the observation site brought higher rBC loadings with more thick coatings and larger core sizes. The mean VED of the rBC presented a significant linear correlation with the number fraction of thickly coated rBC, extrapolating to be  $\sim 150 \text{ nm}$  for the completely non-coated or thinly coated rBC. It was considered as the typical mean VED of the rBC from local traffic sources in this study. Local traffic

was estimated to contribute 35 to 100% of the hourly rBC mass concentration with a mean of 59% during the campaign. Lower local traffic contributions were observed during polluted periods, suggesting increasing contributions from other sources (e.g., coal combustion and biomass burning) to the rBC. Thus, the heavy pollution in Beijing was greatly influenced by other sources in addition to the local traffic.

## 1 Introduction

Black carbon (BC), the major light-absorbing chemical component in atmospheric aerosols, plays an important role in the radiative balance of the earth system through its direct effect of heating the lower atmosphere and indirect effect of affecting cloud properties (Ramanathan and Carmichael, 2008). Although BC is hydrophobic, it can still act as a cloud condensation nucleus when internally mixed with hydrophilic chemical compounds (Zhang et al., 2008a) and thus indirectly affect cloud properties and associated radiative budget (Ramanathan et al., 2001). BC aerosols thus have a great impact on regional and global climate and weather (Menon et al., 2002; Ramanathan and Carmichael, 2008; Ding et al., 2013; Liao and Shang, 2015; Huang et al., 2016). BC can also increase atmospheric stability by its heating effect in the

lower troposphere and cooling role at the surface (Wang et al., 2013), which in turn suppresses the diffusion of pollutants, deteriorates air quality and enhances haze weather intensity (Ding et al., 2016). However, quantifying BC's impact on radiative forcing and environment is challenging and has large uncertainties because of the large variations in its concentration and physicochemical properties (IPCC, 2013). The light absorption of BC highly depends on its size distribution and morphology. Mie calculations for hypothetical BC spheres show that the mass absorption cross sections reach their peaks at a diameter of  $\sim 150$  nm and then decrease sharply with further increases in size (see Fig. 4 in Bond and Bergstrom, 2006). However, atmospheric BC particles apparently consist of aggregates of small primary spherules  $\sim 15$  to 60 nm in diameter (Alexander et al., 2008; Zhang et al., 2008a). They are chain agglomerates when freshly emitted from the combustion sources, resulting in increasing mass-normalized absorption with the particle mobility size (Khalizov et al., 2009). These fresh BC particles are quickly coated by other aerosol components in the atmosphere, leading to the collapse of the chain agglomerates into more compact BC cores (Zhang et al., 2008a). An alteration in the morphology of BC due to a thin coating causes competition between light absorption enhancement and decline, resulting in little variation in the absorption efficiency (Wang et al., 2013; Peng et al., 2016). Subsequently, the thickened coating of the scattering shell enclosing the compact BC cores enhances the light absorption of BC by the lensing effect, although the upper limit of the enhanced amplitude varied among different studies (e.g., Schnaiter et al., 2005; Shiraiwa et al., 2010; Khalizov et al., 2009; Peng et al., 2016).

With its rapid economic development, China has been suffering from heavy air pollution (Yin and Wang, 2016). Annual BC emissions to the atmosphere in China are very high, accounting for approximately half of the total emissions in Asia and one-fifth globally (Qin and Xie, 2012). Existing studies on ambient BC mostly focused on its mass concentrations (e.g., Cao et al., 2007; Zhang et al., 2008b), and little is known about its physicochemical properties, including size, morphology and mixing state (e.g., Huang and Yu, 2008; Cheng et al., 2012), mainly due to the limitations of the measurement methodology. A traditional approach to determining BC size distribution is through analyzing the BC mass of size-segregated aerosol samples (Huang and Yu, 2008; Yu et al., 2010), which provides size information of BC-containing particles because BC particles are frequently internally mixed with other aerosol components in the atmosphere (Shiraiwa et al., 2007; Schwarz et al., 2008). The time resolution in this approach typically ranged from hours to days. In the most recent decade, a novel analyzer, single-particle soot photometer (SP2), has been developed, which can measure the mass and size of the refractory BC (rBC) in high time resolution (Stephens et al., 2003; Schwarz et al., 2006). The mixing state of rBC particles can also be derived from the measurement of SP2 (Gao et al., 2007; Moteki and

Kondo, 2007, 2008; Laborde et al., 2012). Measurements of the sizes and mixing states of rBC based on this technology has been limited to a few regions in China (e.g., Huang et al., 2012; Wang et al., 2014a, 2015a; Wu et al., 2016; Gong et al., 2016), as the SP2 is very expensive and its performance is limited (Gysel et al., 2012; Liggio et al., 2012). It should be noted that the sizes of rBC reported by SP2 are generally mass-equivalent diameters rather than mobility- or aerodynamic-based ones, which are determined on the basis of the mass measurements of individual rBC-containing particles. Thus, they are independent of the morphology or mixing.

Although the physicochemical properties of BC in the atmosphere are greatly diverse, its mass-equivalent sizes should vary little during their typical lifetime in the atmosphere ( $\sim 1$  week) since BC itself is chemically inert under ambient conditions. In other words, the mass-size of a BC particle is independent of its morphology and mixing state, although coating with other components will reduce its mobility diameter and enlarge the size of the mixed particle in which the BC is embedded. As it is a byproduct of the incomplete combustion of fossil fuels and biomass, the BC size should be highly dependent on the emission sources, including fuel type and combustion condition. Based on the measurement by SP2, Liu et al. (2014) showed smaller sizes of the rBC cores from traffic than those from solid fuel sources and attributed the rBC concentrations from the two dominant sources accordingly. The rBC sizes measured at rural or remote sites were considerably larger than those measured at urban sites (Huang et al., 2012; Schwarz et al., 2013), implying that smaller sizes of rBC are emitted from traffic sources. Combining the measurement of SP2 and the chemical source apportionment of daily PM<sub>2.5</sub> samples, Wang et al. (2016) showed that the rBC from biomass burning and coal combustion had larger mass-equivalent diameter than that from traffic.

Influenced by the local emissions (e.g., traffic exhaust) as well as regional transport of air pollutants from the surrounding heavily polluted areas, the physicochemical properties of ambient BC aerosols in urban Beijing are highly varied. In this study, the mass-equivalent size distributions of rBC were first revealed in urban Beijing based on the SP2 measurement during a wintertime in 2014 when haze occurred frequently. The variations in the rBC size were also investigated, accompanied by an analysis of its relation with aerosol chemical composition and its potential source contributions. In the present study, a novel approach was employed to evaluate the contribution of local traffic to the rBC concentration based on the measured rBC sizes and reasonable assumptions, including a deductive mean diameter of rBC from local traffic and relatively stable rBC sizes in the air masses transported over certain regions.

## 2 Methodology

In situ measurements of rBC were conducted using a SP2 (Droplet Measurement Technology, Inc., Boulder, CO, USA) on the rooftop (approximately 8 m above ground level) of an experimental building at the Tower Division of the Institute of Atmospheric Physics, Chinese Academy of Sciences (39°58' N, 116°22' E), during a late winter period from 24 February to 15 March 2014, before the residential heating season ended. The SP2 directly detects the incandescent intensity of an individual rBC-containing particle when it passes through an intra-cavity Nd:YAG laser beam with a Gaussian distribution (Schwarz et al., 2006). The incandescent intensity is converted to the mass of rBC based on the calibration of incandescent signals of size-selected soot standards performed pre- and post-sampling. In this study, the Aquadag (Acheson, Inc., USA) was used as a reference rBC and size-selected by a scanning mobility particle sizer spectrometer (SMPS; TSI, Inc., Shoreview, MN, USA) for calibration. Compared to the ambient rBC, it is more sensitive to the incandescence signal. Thus, a scaling factor of 0.75 is employed with the calibration curve to induce more reliable rBC mass determinations (Baumgardner et al., 2012; Laborde et al., 2012). Moreover, an approximately 10 % underestimation of the SP2-derived bulk rBC mass concentration due to the detection limitations outside the rBC mass range of  $\sim 0.3$ – $120$  fg was considered (Wang et al., 2014a, 2015a). The total uncertainty in the rBC mass determination was  $\sim 25$  %, including the uncertainties inherent in the mass calibration, flow measurement and estimation of BC masses beyond the SP2 detection range (Wu et al., 2016). The scattering signal is synchronously detected by the SP2 and used to determine the optical size of a single particle (Gao et al., 2007; Laborde et al., 2012). In this study, the scattering signal was employed to distinguish the mixing state of rBC-containing particles. A traditional method based on the delay time between the incandescent and scattering peaks was utilized to distinguish the rBC cores with and without a thick coating (Schwarz et al., 2006; Moteki and Kondo, 2007; Wang et al., 2014a; Wu et al., 2016). The rBC-containing particles were defined as either thickly coated or uncoated to thinly coated according to the distribution of detected lag times, which was bimodal and had a local minimum at  $2 \mu\text{s}$  (Fig. S1 in the Supplement). We defined the rBC particles as thickly coated if the lag times were longer than  $2 \mu\text{s}$ . On this basis, the number fraction of thickly coated rBC ( $\text{NF}_{\text{coated}}$ ), defined as the ratio of the number of thickly coated rBC particles to that of all detectable rBC particles, was calculated to characterize the relative mixing extent of the BC aerosols in different ambient samples. A similar measurement was conducted in January 2013, and more details of the experimental setup and data process can be found in Wu et al. (2016).

Samples of  $\text{PM}_{2.5}$  were collected twice a day during this campaign, each lasting for 12 hours. The chemical contents including organic carbon (OC), elemental carbon (EC),

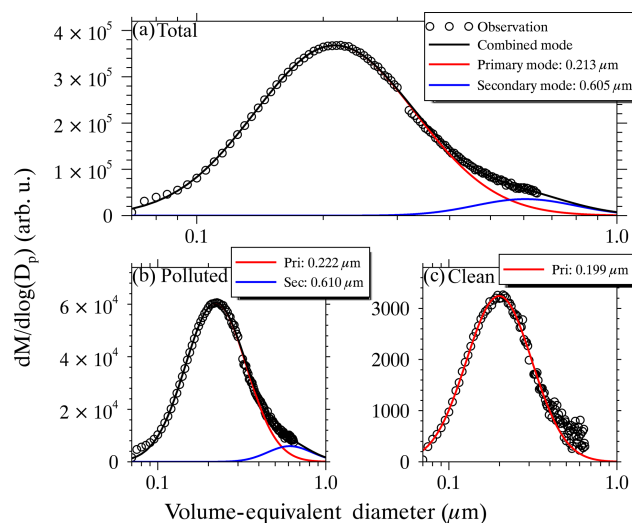


**Figure 1.** Size distributions of rBC in volume-equivalent diameter during a campaign from 24 February to 15 March, 2014. The red and blue lines are the lognormal fittings to the primary and secondary modes, respectively, and the black ones correspond to the combined mode.

water-soluble ions (e.g.,  $\text{SO}_4^{2-}$ ,  $\text{NO}_3^-$ , and  $\text{NH}_4^+$ ) and trace elements were analyzed in the laboratory, as presented in detail by Lin et al. (2016).

## 3 Results and discussion

### 3.1 Size distribution of rBC and its variation

As shown in Fig. 1, the mass of rBC ( $dM / d\log D_p$ ) exhibited an approximately lognormal distribution as a function of the volume-equivalent diameter (VED) of void-free rBC, as has been commonly observed (e.g., Schwarz et al., 2006; Huang et al., 2012; Wang et al., 2016). The similar size distribution was also observed in our previous campaign in January 2013 (Fig. S2 in the Supplement). A minor mode was also captured at large sizes (peaked at  $\sim 600$  nm), only accounting for  $\sim 6$  % of the SP2-determined rBC masses. An analogous minor mode was previously observed at other sites in China. Huang et al. (2011) reported a minor peak with a diameter of  $\sim 690$  nm at Kaiping, a rural site in the Pearl River Delta (PRD) region of China. Wang et al. (2014b) found a minor peak with a diameter of  $\sim 470$ – $500$  nm in a remote area of the Qinghai–Tibetan Plateau and considered it a likely feature of the rBC distribution of biofuel and/or open-fire burning sources, which needs further verification using measurements of the size distributions at the emission sources. The peak diameter of the primary mode, with a value of 213 nm, during the campaign is well within the range ( $\sim 150$ – $230$  nm) presented by previous studies conducted in different regions (Huang et al., 2012 and references therein). It should be noted that the density of the assumed

void-free rBC was set to  $1.8 \text{ g cm}^{-3}$  in calculating the VED from the rBC masses measured in this study, which should result in larger VED values compared to those based on the density of  $2.0 \text{ g cm}^{-3}$  used in previous studies. If the density of  $2.0 \text{ g cm}^{-3}$  was employed, the peak diameter of the primary mode would be  $\sim 206 \text{ nm}$  in this study. This value is very close to those observed in urban areas throughout China, e.g.,  $210 \text{ nm}$  in Shenzhen in southern China (Huang et al., 2012),  $205 \text{ nm}$  in Xi'an in western China (Wang et al., 2015b) and  $\sim 200 \text{ nm}$  in Shanghai in eastern China (Gong et al., 2016). The relatively similar mass-size distributions of rBC suggest that there were similar dominant emission sources in different urban regions in China, where vehicle exhaust was one of the important sources emitting rBC particles. Compared to those measured at rural sites in the PRD region in southern China (e.g.,  $220\text{--}222 \text{ nm}$ ; Huang et al., 2011, 2012), the peak diameters of rBC in urban areas are significantly smaller. This might be related to the greater amounts of coal combustion and biomass burning around the rural sites (Huang et al., 2012). In contrast, the sizes of the rBC were much smaller in remote regions, e.g., with a peak diameter of  $\sim 175\text{--}188 \text{ nm}$  in the Qinghai–Tibetan Plateau area (Wang et al., 2014b, 2015a). Wang et al. (2015a) attributed this smaller peak diameter value to the source and considered that biomass burning generated a small rBC with peak VED values in the range of  $\sim 187\text{--}193 \text{ nm}$ . Another important reason for the smaller rBC measured in remote regions, in our opinion, is that more large rBC particles are deposited during their long-range transport to the observation site. Further research on the sizes of rBC from different sources is needed.

The mass-size distributions of rBC during a polluted day (25 February) and a clean one (4 March) are also compared in Fig. 1. The average mass concentrations of rBC ( $\text{MC}_{\text{rBC}}$ ) were  $7.6$  and  $0.4 \mu\text{g m}^{-3}$ , respectively, on the polluted and clean days. The size distribution of rBC during the polluted day is similar to that during the entire observation period, although a larger peak diameter was observed, with a value of  $221 \text{ nm}$ . In contrast, the peak diameter on the clean day is obviously smaller, with a value of  $199 \text{ nm}$ . The secondary mode cannot be well characterized on the clean day. As mentioned above, the mass-sizes of rBC emitted from a certain source change little during their lifetime in the atmosphere. Thus, the considerable discrepancy of the rBC sizes illustrates significant source alteration during the polluted period compared to that on a clean day. Sun et al. (2014) used the measurements of ACSM at an urban site in Beijing to show that the regional contribution to the BC exceeded  $50\%$  during heavily polluted periods in January 2013. Model simulation also revealed that regional transport contributed an average of  $56\%$  to the  $\text{PM}_{2.5}$  in Beijing in January 2013 when the hazes occurred frequently, and was even higher during polluted periods (Li and Han, 2016). Accordingly, regional transport might play an important role in the increase in rBC sizes during polluted periods in urban Beijing. By compari-

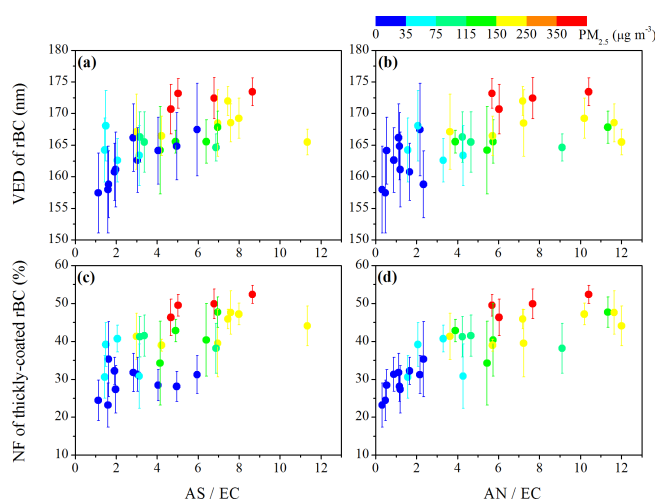


**Figure 2.** Variation in the average volume-equivalent diameters of rBC ( $\text{VED}_{\text{rBC}}$ ) as a function of the mass ratios of (a) ammonium sulfate (AS) and (b) ammonium nitrite (AN) to elemental carbon (EC). The same apply for (c) and (d), but for the number fraction of thickly coated rBC ( $\text{NF}_{\text{coated}}$ ). The vertical bar denotes one standard deviation. The color scale represents the pollution levels defined as the  $\text{PM}_{2.5}$  mass concentration according to the AQI standard of MEP of China.

son, traffic emissions should be the dominant source of rBC on the clean day, contributing to smaller rBC sizes.

The variation in the VED of the rBC is further investigated by comparing the mean VED value of rBC ( $\text{VED}_{\text{rBC}}$ ) with the mass ratios of secondary inorganic components (i.e., ammonium sulfate, AS; ammonium nitrite, AN) to EC, a representation of the aerosol aging degree. What should be noted is that the mass concentrations of AS were calculated from those of sulfate multiplying by a factor of 1.375, and those of AN were from nitrate multiplying by a factor of 1.29, according to the molecular weight, because the aerosol samples were almost neutral in ionic equilibrium (Fig. S3). Generally, the average  $\text{VED}_{\text{rBC}}$  positively correlated with AS/EC and AN/EC ratios, with correlation coefficients of  $0.63$  ( $p < 0.01$ ) and  $0.61$  ( $p < 0.01$ ), respectively (Fig. 2a and b). Higher AS/EC and AN/EC ratios were observed in polluted samples, corresponding to higher  $\text{VED}_{\text{rBC}}$  during these periods.

It is interesting to note that the  $\text{VED}_{\text{rBC}}$  correlated more closely with the AS/EC ratio than AN/EC, especially under a clean condition. The correlation coefficient between  $\text{VED}_{\text{rBC}}$  and AS/EC is  $0.88$  ( $p < 0.01$ ) during clean periods, with  $\text{PM}_{2.5}$  mass concentrations lower than  $35 \mu\text{g m}^{-3}$  (blue dots in Fig. 2), much higher than that between  $\text{VED}_{\text{rBC}}$  and AN/EC. By contrast, the  $\text{NF}_{\text{coated}}$  varied less with AS/EC during these periods (Fig. 2c). This means that a higher AS/EC had less effect on the fraction of thickly coated rBC during these clean periods but was related to larger rBC sizes, which were highly dependent on the emission sources. In

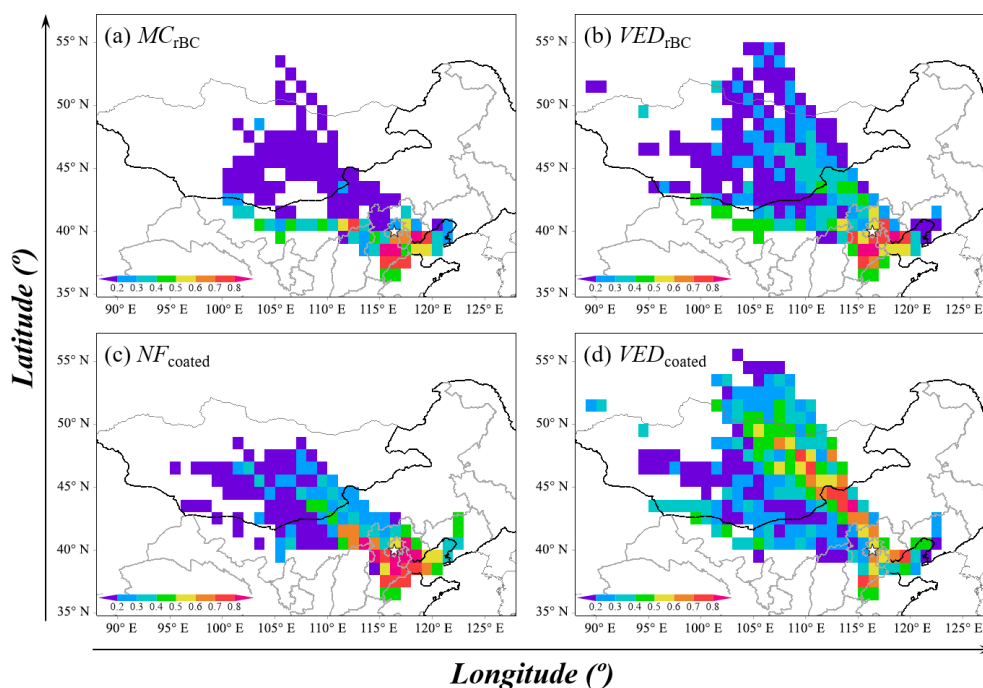


**Figure 3.** Distributions of gridded ( $1^\circ \times 1^\circ$ ) potential source contribution functions of (a) mass concentration (MC) and (b) volume-equivalent diameter (VED) of rBC as well as (c) number fraction (NF) and (d) VED of thickly coated rBC. The overlaid star symbol represents the geographical location of the observation site.

other words, higher AS/EC values might indicate an increasing contribution of sources other than traffic producing larger rBC, as sulfur is one of the major trace elements of coal combustion but not of traffic (Zhang et al., 2013; Wang et al., 2016). However,  $NF_{\text{coated}}$  was highly related to AN/EC, with a correlation coefficient of 0.81 ( $p < 0.01$ ) during the clean periods (Fig. 2d). Even considering the entire samples, the correlation coefficient between  $NF_{\text{coated}}$  and AN/EC was as high as 0.81 ( $p < 0.01$ ), much higher than that (0.65,  $p < 0.01$ ) between  $NF_{\text{coated}}$  and AS/EC. This implies that the mixing state of rBC is much more sensitive to AN/EC in urban Beijing, especially during the clean periods. The secondary formation of AN might play an important role in the coating processes of rBC but have a negligible effect on the core size of the rBC.

### 3.2 Potential source contribution to rBC mass and size

The potential source contribution function (PSCF) analysis, based on hourly resolved 48 h backward trajectories arriving at the observation site 100 m above ground level, was performed using TrajStat software (Wang et al., 2009). The threshold of the PSCF analysis was set to the mean value of each variable. A weight function on the gridded PSCF values was employed on those cells that have few trajectory endpoints (Wang et al., 2006). Generally, the areas east and south of the observation site had the largest number of potential source regions of high rBC concentrations, with weighted

PSCF (WPSCF) values of  $MC_{\text{rBC}}$  larger than 0.7 (Fig. 3a). Previous studies showed that Hebei province, on the southern and eastern borders of Beijing, was a major contributor to pollutants in Beijing, as its industrial activities are intense (Zhang et al., 2013). The high coal consumption associated with the heavy industrial activities and residential heating in the cold season should be an important source of high atmospheric rBC loading in these areas. Similarly, the distribution of the WPSCF values of  $VED_{\text{rBC}}$  shows that the eastern and southern regions are also correlated with large  $VED_{\text{rBC}}$  values (Fig. 3b). This implies that the pollution sources in these regions, e.g., heavy industrial activities and residential heating, tend to produce highly concentrated rBC-containing particles with large rBC core sizes. The source apportionment of rBC aerosols in London, based on in situ SP2 measurements, showed that rBC-containing particles from solid fuel sources (coal combustion and biomass burning) had significantly larger rBC cores than those from traffic (Liu et al., 2014). Thus, the high WPSCF values of  $MC_{\text{rBC}}$  and  $VED_{\text{rBC}}$  in the east and south might highly correlate to anthropogenic coal and/or biomass combustion in these regions.

The spatial distribution of the WPSCF values of  $NF_{\text{coated}}$  is shown in Fig. 3c. Associated with the aging processes that increase the thickly coating states of rBC-containing particles through heterogeneous reactions, the WPSCF values of  $NF_{\text{coated}}$  are generally high in the areas surrounding the observation site. It should be noted that higher WPSCF values of  $NF_{\text{coated}}$  ( $> 0.7$ ) dominate in the east to south. In addition



to the transport of thickly coated BC particles from these regions, aging processes of locally emitted BC particles (e.g., from traffic sources) under the southerly-wind-dominant condition, in which the relative humidity (RH) is high (Zhang et al., 2015; Zheng et al., 2015), also increase the fraction of thickly coated rBC (Wu et al., 2016). Although northerly–northwesterly winds also blow in aged rBC-containing particles with thick coatings, the larger amounts of non-coated or thinly coated BC particles from local sources during these periods diminished the WPSCF values of  $NF_{\text{coated}}$  in the north to west regions of the observation site. The low RH and strong winds from these directions are unfavorable to the coating processes of locally emitted fresh rBC particles.

The  $VED_{\text{coated}}$ , defined as the VED of those thickly coated rBC cores, shows a dispersive WPSCF distribution (Fig. 3d). Compared to the distribution of  $VED_{\text{rBC}}$  with high WPSCF values that dominate in the east to south, high WPSCF values of  $VED_{\text{coated}}$  are located in the northern pathway of air masses being transported to the observation site as well. This implies that the regional transport of air masses brings large rBC, no matter which direction it comes from. Dominated by the locally emitted small rBC, the WPSCF values of  $VED_{\text{rBC}}$  are low in the northern region. It further illuminates that local sources such as traffic emit small rBC, while regional transport brings in large rBC. On the basis of the large discrepancy in rBC sizes between local traffic and regional transport generated particles, it is possible to extract the contribution of local traffic emissions from the mixed rBC sources.

## 4 Discussion

### 4.1 Relationship between rBC size and mixing state

As large rBC sizes are usually accompanied by significant contributions of regional transport, which also lead to a high fraction of thickly coated rBC, the  $VED_{\text{rBC}}$  is directly compared with the  $NF_{\text{coated}}$ , as shown in Fig. 4. The two-dimensional histogram of the 5 min average  $VED_{\text{rBC}}$  and  $NF_{\text{coated}}$  presents a significant linear correlation between the two variables. It is characterized more clearly by the variation in the mean  $VED_{\text{rBC}}$  values averaged in increased  $NF_{\text{coated}}$  bins with a resolution of 2 % (magenta circles in Fig. 4). The observed minimum value of the 5 min  $NF_{\text{coated}}$  is  $\sim 10\%$ , representing that there is little pure external mixing of rBC in the atmosphere, even for short periods. However, an assumed mean VED of completely non-coated or thinly coated rBC is extrapolated from the linear curve to  $NF_{\text{coated}}$  with a value of 0 % (i.e., the  $y$ -intercept value). This inferred VED, with a value of  $\sim 150$  nm, might be considered as the typical mean VED of freshly emitted rBC from vehicle exhaust, which has little coating (Zhang et al., 2008a; Peng et al., 2016). It is almost the same as the mean VED of observed rBC without or with thin coating ( $149.5 \pm 4.5$  nm; Fig. S4 in the Supplement). Since these non-coated or thinly coated

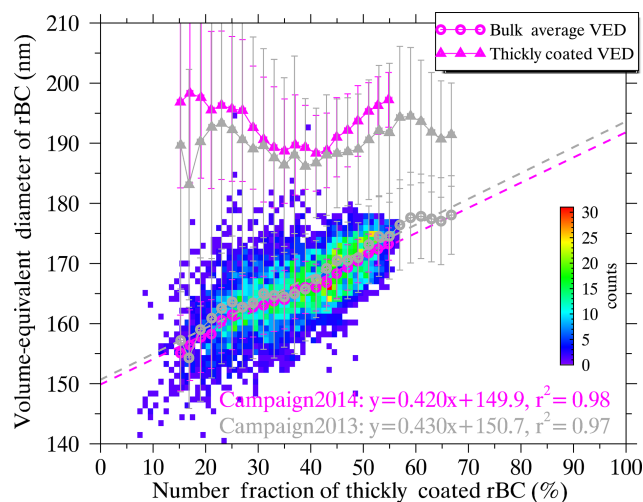


**Figure 4.** Two-dimensional histogram of the 5 min average volume-equivalent diameter of rBC ( $VED_{\text{rBC}}$ ) against number fraction of thickly coated rBC ( $NF_{\text{coated}}$ ) during the campaign in the late winter in 2014. The magenta circles and triangles with error bars represent the mean  $VED_{\text{rBC}}$  and VED of thickly coated rBC ( $VED_{\text{coated}}$ ) averaged in each  $NF_{\text{coated}}$  bin with a resolution of 2 %, respectively. The dashed magenta line denotes the linear regression of  $VED_{\text{rBC}}$  against  $NF_{\text{coated}}$ . The relationship between  $VED_{\text{rBC}}$  and  $NF_{\text{coated}}$  during another campaign in January 2013 (Wu et al., 2016) is comparatively overlapped in gray.

rBC are mostly from local traffic sources in urban Beijing where the major industrial sources are few, the consistency in the inferred and mean VED of non-coated or thinly coated rBC verifies the rationality of our deduction here. We are surprised to find that the linear relationship between  $VED_{\text{rBC}}$  and  $NF_{\text{coated}}$  seems to be common, as was also found in another campaign conducted in January 2013 (Wu et al., 2016; gray circles in Fig. 4). More observations are needed to further verify this relationship. According to the results presented in this study, a mean VED of  $\sim 150$  nm is legitimately accepted as the typical SP2-determined mean VED of fresh rBC from local traffic sources. Size-segregated aerosol samples also revealed a mode peaked at  $\sim 150$  nm in aerodynamic diameter for elemental carbon in urban Guangzhou, a megacity in the PRD region, attributed to the traffic emissions (Yu and Yu, 2009; Yu et al., 2010). A second mode at diameter of  $\sim 400$  nm was also observed and was also thought to be associated with the traffic emission (Yu and Yu, 2009). In contrast, only the smaller EC mode with peak diameter in the range of 100–200 nm was observed from traffic sources in urban areas of developed counties (Allen et al., 2001; Kleeman et al., 2000). To date, no literature is available for comparison with the case in Beijing because of the limitation in characterizing the size distribution of EC at the small mode (e.g.,  $< 400$  nm). Considering the stringent fuel and vehicle emission standards implemented in Beijing, the VED of  $\sim 150$  nm for local traffic sources is reasonable, al-

though further measurement studies are still needed to verify this. As mentioned above, the VED of certain rBC varies little once it is emitted to the atmosphere. Thus, the mean VED with a value of  $\sim 150$  nm was employed in this study as being representative of the rBC size from local traffic.

The variation in  $VED_{\text{coated}}$  with  $NF_{\text{coated}}$  is also shown (magenta triangles in Fig. 4). It is interesting to find that, compared to  $VED_{\text{rBC}}$ ,  $VED_{\text{coated}}$  presents a fluctuant variation as  $NF_{\text{coated}}$  increases. The larger  $VED_{\text{coated}}$  at lower  $NF_{\text{coated}}$  is comprehensible because regionally transported large rBC dominates in the thickly coated rBC particles, and the small rBC from local traffic is mainly externally mixed with other aerosol components at this stage. As the  $NF_{\text{coated}}$  increases from 10–20 to 30–40 %, the mean  $VED_{\text{coated}}$  gradually decreases from  $\sim 200$  nm to  $\sim 190$  nm. This implies that some small rBC (e.g., rBC from local traffic) contributes a considerable portion of the thickly coated rBC particles at this stage. In addition to the influence of the emission sources on the rBC size, this decrease in  $VED_{\text{coated}}$  can also be explained by the contamination of the local traffic-emitted small rBC into the thickly coated rBC particles through atmospheric aging processes (i.e., coating with other components). It should be noted that the  $VED_{\text{rBC}}$  sustained increases at this stage, implying that other sources besides the local traffic also brought large rBC at the same time. This is because if the increase in  $NF_{\text{coated}}$  only results from the coating processes of the local traffic-emitted rBC, the VED of the entire rBC (i.e.,  $VED_{\text{rBC}}$ ) should vary little. The  $VED_{\text{coated}}$  increases significantly when  $NF_{\text{coated}}$  exceeds 40 %, suggesting that regional transport dominates at this stage, bringing a large amount of thickly coated rBC particles with a large rBC core. Meanwhile, the mean  $MC_{\text{rBC}}$  increases dramatically from  $1.3$  to  $5.0 \mu\text{g m}^{-3}$  when  $NF_{\text{coated}}$  increases from 30 to 50 %, further confirming the great contribution of regional transport to the rBC at this stage. By comparison, the mean rBC concentration varies in a small range of  $0.8$ – $1.4 \mu\text{g m}^{-3}$  when  $NF_{\text{coated}}$  is lower than 30 %. The observation from the campaign of 2013 showed a similar variation in  $VED_{\text{coated}}$  against  $NF_{\text{coated}}$  (gray triangles in Fig. 4).

#### 4.2 Extracting the local traffic contribution to rBC

As  $VED_{\text{rBC}}$  with a value of  $\sim 150$  nm is expected to be the typical mean VED of the local traffic-emitted rBC and varies little in the atmosphere, it provides the possibility of extracting the contribution of the local traffic to the rBC from the total rBC mass concentration according to the variation in  $VED_{\text{rBC}}$ . However, the typical mean VED of rBC from other sources, such as coal combustion and biomass burning, is difficult to identify. It depends on many factors, including fuel type and combustion condition. In this study, a simple assumption was employed to identify the typical mean VED of rBC from other sources besides local traffic according to where the air masses came from. During a short period when the source emissions were relatively stable, the rBC from a

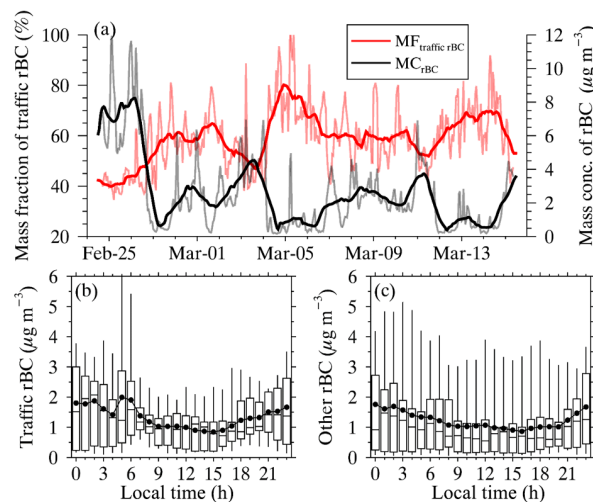


**Figure 5.** (a) Time series of hourly mass concentration of rBC ( $MC_{\text{rBC}}$ ) and mass fraction of local traffic-related rBC ( $MF_{\text{traffic}}$ ). The bold lines represent the variations of the daily moving averaged  $MC_{\text{rBC}}$  and  $MF_{\text{traffic}}$ . Panels (b) and (c) show the diurnal variations in the decomposed rBC from local traffic emission and other sources, respectively.

certain direction was assumed to have a certain mean VED, no matter from which source it is emitted. Thus, a cluster analysis was performed on the 48 h backward trajectories that arrived at the observation site. Five clusters were identified using TrajStat software according to the total spatial variation in the cluster numbers (as shown in Fig. S5). As the rBC tends to be thickly coated in the regionally transported air masses, the mean VED of the rBC from sources other than local traffic was derived from the values of  $VED_{\text{coated}}$ . The local traffic-emitted small rBC can also become thickly coated through aging processes in the atmosphere, so a further assumption is employed to consider the VED of rBC from other sources to be equal to the mean value of the upper 5 % percentile of  $VED_{\text{coated}}$  in each cluster. Five typical mean VEDs of rBC from sources other than local traffic were identified, with values in the range of 195.5–208.3 nm (Fig. S5). Such simple assumptions might induce large uncertainties in the absolute contribution of the local traffic to the rBC, but it should well reflect the variation in the traffic contribution.

Using a multiple linear regression to  $VED_{\text{rBC}}$ , the hourly-resolved traffic contribution to the rBC was extracted on the basis of the derived VED of the rBC from local traffic and other sources. The mass fraction of the traffic-induced rBC ( $MF_{\text{traffic}}$ ) is shown in Fig. 5a (red line). During this campaign, approximately 35 to 100 % of the hourly  $MC_{\text{rBC}}$  is attributed to local traffic emissions, with a mean of 59 %. Although the carbon isotope analysis is commonly used in the source identification EC (Zhang et al., 2015; Liu et al., 2016), it is difficult to distinguish the traffic-related source from other fossil-fuel combustion sources. Based on a multi-

ple linear regression analysis of the contributions of the three dominant factors (i.e., traffic, coal combustion and biomass burning) to the rBC derived from the chemical source apportionment of the daily PM<sub>2.5</sub> samples, Wang et al. (2016) showed a slightly lower contribution of the traffic to the rBC in urban Xi'an, with a mean of 46 % and a daily contribution in the range of 0.8 to 77.2 %. Since entirely different methods were employed in addition to the different locations, the resolved traffic contribution to the rBC should not be compared absolutely. However, the relatively lower MC<sub>rBC</sub> in this study (with a mean of 2.8 μg m<sup>-3</sup> compared to 8.0 μg m<sup>-3</sup>) might partly interpret the slightly higher contribution of traffic, as a lower MC<sub>rBC</sub> is usually accompanied by a higher contribution of the local traffic. It is clear that MF<sub>traffic</sub> is negatively correlated with MC<sub>rBC</sub>, with the correlation coefficient as high as -0.84 ( $p < 0.01$ ) between the daily moving averaged MF<sub>traffic</sub> and MC<sub>rBC</sub> (Fig. 5a). This means that the traffic contribution to the rBC decreased significantly during the polluted periods when the rBC loading increased. In other words, the rBC from other sources such as coal combustion and biomass burning played an increased role in these polluted periods. This implies that the high MC<sub>rBC</sub> in urban Beijing was not only due to the accumulation of the local traffic emissions during stable synoptic conditions but can also be attributed to the overlaying pollution from other sources.

The diurnal variations of the decomposed MC<sub>rBC</sub> from local traffic and other sources are shown in Fig. 5b and c, respectively. A common diurnal variation in MC<sub>rBC</sub> with high values during the nighttime and low ones in the daytime is shown for rBC produced by both the traffic and other sources, suggesting the important impact of the mixing layer height on the surface MC<sub>rBC</sub>. A high mixing layer in the daytime, especially in the afternoon, favors the diffusion of the pollutants, leading to a low value of MC<sub>rBC</sub>. A low mixing layer in the nighttime suppresses the diffusion of pollutants, resulting in a high value of MC<sub>rBC</sub>. It is noted that a significant peak MC<sub>rBC</sub> of local traffic was observed in the early morning (05:00–06:00 LT). Moreover, the increase in the local traffic-related MC<sub>rBC</sub> occurs earlier than that of other sources in the evening. It corresponds well to the increased traffic contribution in the morning and evening rush hours. Although the traffic flow showed a significant decrease in the nighttime, a dramatic increase in the flow of heavy-duty diesel vehicles was observed due to Beijing's traffic regulations (Song et al., 2013). These vehicles have much higher emission factors of BC (~15–30 times) than light-duty gasoline vehicles, and thus play a non-negligible role in the high MC<sub>rBC</sub> values around midnight. Generally, the diurnal variation of MC<sub>rBC</sub> verifies to some degree the rationality of the method we employed to distinguish the contribution of the local traffic emission from that of other sources.

## 5 Summary and concluding remarks

An approximate lognormal size distribution of the rBC in volume-equivalent diameter was observed in urban Beijing during a polluted winter in 2014, based on measurements using a SP2. The peak diameter was 213 nm, assuming void-free rBC with a density of 1.8 g cm<sup>-3</sup>, which is close to the values observed in other urban areas in China. The measured sizes of the rBC were considerably larger during the polluted period than clean period, implying a source variation of the rBC. The mean VED<sub>rBC</sub> positively correlated with the ratios of secondary inorganic aerosols (including AS and AN) to EC, especially the ratio of AS / EC under a clean condition. This implies that the rBC sizes are highly related to the emission sources because sulfur is one of the major trace elements in coal combustion, while little is emitted from traffic. By comparison, the mean NF<sub>coated</sub> correlated more with AN / EC, implying the important effect of the secondary formation of nitrate on the rBC mixing state. The PSCF analysis showed that regional transport from the east to south of Beijing was a major source of high rBC loading in Beijing and was accompanied by a large VED<sub>rBC</sub> and high NF<sub>coated</sub>.

A significant positive correlation existed between VED<sub>rBC</sub> and NF<sub>coated</sub>, inferring the typical mean VED of the rBC from local traffic, with a value of 150 nm. Based on the inferred VED and further reasonable assumptions, the local traffic contribution to the rBC was extracted. Local traffic emissions played an important role in the rBC loading in urban Beijing and contributed 59 % of the MC<sub>rBC</sub> on campaign average. However, its contribution decreased significantly in the polluted period compared to the clean period. A significant negative correlation is found between the daily moving average MC<sub>rBC</sub> and MF<sub>traffic</sub> with a coefficient of -0.87. A similar diurnal variation in the decomposed MC<sub>rBC</sub> associated with local traffic and other sources was observed with high values in the nighttime and low values in the daytime. However, a significant increase in traffic MC<sub>rBC</sub> was observed in the early morning and evening, indicating the increased contribution of local traffic emissions. Despite potential large uncertainties in the estimated contribution from the local traffic to rBC, due to the many assumptions employed, its relative variation is clearly demonstrated. Further research measuring sizes of rBC directly from various sources, including coal combustion, biomass burning and traffic exhaust, is needed to validate the findings presented in this study. This work provides a relatively simple but novel method of extracting the contribution of the local traffic to the rBC on the basis of the size measurement of the rBC in the atmosphere, which could enhance source apportionment research in urban Beijing and other areas where air pollution is severe.

*Data availability.* Raw data are archived at the Institute of Atmospheric Physics, Chinese Academy of Sciences, and are available on request by contacting the corresponding authors.



The Supplement related to this article is available online at <https://doi.org/10.5194/acp-17-7965-2017-supplement>.

*Competing interests.* The authors declare that they have no conflict of interest.

*Acknowledgements.* This work was supported by the National Natural Science Foundation of China (no. 91644217, 41575150 and 41305128), the Special Scientific Research Funds for Environment Protection Commonweal Section (no. 201409027) and the Jiangsu Collaborative Innovation Center for Climate Change.

Edited by: Imre Salma

Reviewed by: two anonymous referees

## References

- Alexander, D. T. L., Crozier, P. A., and Anderson, J. R.: Brown carbon spheres in East Asian outflow and their optical properties, *Sciences*, 321, 833–836, 2008.
- Allen, J. O., Mayo, P. R., Hughes, L. S., Salmon, L. G., and Cass, G. R.: Emissions of size-segregated aerosols from on-road vehicles in the Caldecott Tunnel, *Environ. Sci. Technol.*, 35, 4189–4197, 2001.
- Baumgardner, D., Popovicheva, O., Allan, J., Bernardoni, V., Cao, J., Cavalli, F., Cozic, J., Diapouli, E., Eleftheriadis, K., Genberg, P. J., Gonzalez, C., Gysel, M., John, A., Kirchstetter, T. W., Kuhlbusch, T. A. J., Laborde, M., Lack, D., Müller, T., Niessner, R., Petzold, A., Piazzalunga, A., Putaud, J. P., Schwarz, J., Sheridan, P., Subramanian, R., Swietlicki, E., Valli, G., Vecchi, R., and Viana, M.: Soot reference materials for instrument calibration and intercomparisons: a workshop summary with recommendations, *Atmos. Meas. Tech.*, 5, 1869–1887, <https://doi.org/10.5194/amt-5-1869-2012>, 2012.
- Bond, T. C. and Bergstrom, R. W.: Light absorption by carbonaceous particles: an investigative review, *Aerosol Sci. Technol.*, 40, 27–67, 2006.
- Cao, J. J., Lee, S. C., Chow, J. C., Watson, J. G., Ho, K. F., Zhang, R. J., Jin, Z. D., Shen, Z. X., Chen, G. C., Kang, Y. M., Zou, S. C., Zhang, L. Z., Qi, S. H., Dai, M. H., Cheng, Y., and Hu, K.: Spatial and seasonal distributions of carbonaceous aerosols over China, *J. Geophys. Res.*, 112, D22S11, <https://doi.org/10.1029/2006JD008205>, 2007.
- Cheng, Y. F., Su, H., Rose, D., Gunthe, S. S., Berghof, M., Wehner, B., Achtert, P., Nowak, A., Takegawa, N., Kondo, Y., Shiraiwa, M., Gong, Y. G., Shao, M., Hu, M., Zhu, T., Zhang, Y. H., Carmichael, G. R., Wiedensohler, A., Andreae, M. O., and Pöschl, U.: Size-resolved measurement of the mixing state of soot in the megacity Beijing, China: diurnal cycle, aging and parameterization, *Atmos. Chem. Phys.*, 12, 4477–4491, <https://doi.org/10.5194/acp-12-4477-2012>, 2012.
- Ding, A. J., Fu, C. B., Yang, X. Q., Sun, J. N., Petäjä, T., Kerminen, V.-M., Wang, T., Xie, Y., Herrmann, E., Zheng, L. F., Nie, W., Liu, Q., Wei, X. L., and Kulmala, M.: Intense atmospheric pollution modifies weather: a case of mixed biomass burning with fossil fuel combustion pollution in eastern China, *Atmos. Chem. Phys.*, 13, 10545–10554, <https://doi.org/10.5194/acp-13-10545-2013>, 2013.
- Ding, A. J., Huang, X., Nie, W., Sun, J. N., Kerminen, V.-M., Petäjä, T., Su, H., Cheng, Y. F., Yang, X.-Q., Wang, M. H., Chi, X. G., Wang, J. P., Virkkula, A., Guo, W. D., Yuan, J., Wang, S. Y., Zhang, R. J., Wu, Y. F., Song, Y., Zhu, T., Zilitinkevich, S., Kulmala, M., and Fu, C. B.: Enhanced haze pollution by black carbon in megacities in China, *Geophys. Res. Lett.*, 43, 2873–2879, 2016.
- Gao, R. S., Schwarz, J. P., Kelly, K. K., Fahey, D. W., Watts, L. A., Thompson, T. L., Spackman, J. R., Slowik, J. G., Cross, E. S., Han, J.-H., Davidovits, P., Onasch, T. B., and Worsnop, D. R.: A novel method for estimating light-scattering properties of soot aerosols using a modified single-particle soot photometer, *Aerosol Sci. Technol.*, 41, 125–135, 2007.
- Gong, X. D., Zhang, C., Chen, H., Nizkorodov, S. A., Chen, J. M., and Yang, X.: Size distribution and mixing state of black carbon particles during a heavy air pollution episode in Shanghai, *Atmos. Chem. Phys.*, 16, 5399–5411, 2016.
- Gysel, M., Laborde, M., Mensah, A. A., Corbin, J. C., Keller, A., Kim, J., Petzold, A., and Sierau, B.: Technical Note: The single particle soot photometer fails to reliably detect PALAS soot nanoparticles, *Atmos. Meas. Tech.*, 5, 3099–3107, <https://doi.org/10.5194/amt-5-3099-2012>, 2012.
- Huang, X., Ding, A., Liu, L., Liu, Q., Ding, K., Niu, X., Nie, W., Xu, Z., Chi, X., Wang, M., Sun, J., Guo, W., and Fu, C.: Effects of aerosol-radiation interaction on precipitation during biomass-burning season in East China, *Atmos. Chem. Phys.*, 16, 10063–10082, <https://doi.org/10.5194/acp-16-10063-2016>, 2016.
- Huang, X.-F. and Yu, J. Z.: Size distributions of elemental carbon in the atmosphere of a coastal urban area in South China: characteristics, evolution processes, and implications for the mixing state, *Atmos. Chem. Phys.*, 8, 5843–5853, <https://doi.org/10.5194/acp-8-5843-2008>, 2008.
- Huang, X. F., Gao, R. S., Schwarz, J. P., He, L. Y., Fahey, D. W., Watts, L. A., McComiskey, A., Cooper, O. R., Sun, T. L., Zeng, L. W., Hu, M., and Zhang, Y. H.: Black carbon measurements in the Pearl River Delta region of China, *J. Geophys. Res.*, 116, D12208, <https://doi.org/10.1029/2010JD014933>, 2011.
- Huang, X. F., Sun, T. L., Zeng, L. W., Yu, G. H., and Luan, S. J.: Black carbon aerosol characterization in a coastal city in South China using a single particle soot photometer, *Atmos. Environ.*, 51, 21–28, 2012.
- IPCC: Summary for policymakers, in: *Climate Change 2013: The Physical Science Basis. Contribution of Working Group I to the Fifth Assessment Report of the Intergovernmental Panel on Climate Change*, edited by: Stocker, T. F., Qin, D., Plattner, G.-K., Tignor, M., Allen, S. K., Boschung, J., Nauels, A., Xia, Y., Bex, V., and Midgley, P. M., Cambridge University Press, Cambridge, United Kingdom and New York, NY, USA, 2013.
- Khalizov, A. F., Xue, H. X., Wang, L., Zheng, J., and Zhang, R. Y.: Enhanced light absorption and scattering by carbon soot aerosol internally mixed with sulfuric acid, *J. Phys. Chem. A*, 113, 1066–1074, 2009.
- Kleeman, M. J., Schauer, J. J., and Cass, G. R.: Size and composition distribution of fine particulate matter emitted from motor vehicles, *Environ. Sci. Technol.*, 34, 1132–1142, 2000.

- Laborde, M., Mertes, P., Zieger, P., Dommen, J., Baltensperger, U., and Gysel, M.: Sensitivity of the single particle soot photometer to different black carbon types, *Atmos. Meas. Tech.*, 5, 1031–1043, 2012.
- Li, J. W. and Han, Z. W.: A modeling study of severe winter haze events in Beijing and its neighboring regions, *Atmos. Res.*, 170, 87–97, 2016.
- Liao, H. and Shang, J. J.: Regional warming by black carbon and tropospheric ozone: a review of progresses and research challenges in China, *J. Meteor. Res.*, 29, 525–545, 2015.
- Liggio, J., Gordon, M., Smallwood, G., Li, S.-M., Stroud, C., Staebler, R., Lu, G., Lee, P., Taylor, B., and Brook, J. R.: Are emissions of black carbon from gasoline vehicles underestimated? Insights from near and on-road measurements, *Environ. Sci. Technol.*, 46, 4819–4828, 2012.
- Lin, Y.-C., Hsu, S.-C., Chou, C.-C.-K., Zhang, R. J., Wu, Y. F., Kao, S.-J., Luo, L., Huang, C.-H., Lin, S.-H., and Huang, Y.-T.: Wintertime haze deterioration in Beijing by industrial pollution deduced from trace metal fingerprints and enhanced health risk by heavy metals, *Environ. Pollut.*, 208, 284–293, 2016.
- Liu, D., Allan, J. D., Young, D. E., Coe, H., Beddows, D., Fleming, Z. L., Flynn, M. J., Gallagher, M. W., Harrison, R. M., Lee, J., Prevot, A. S. H., Taylor, J. W., Yin, J., Williams, P. I., and Zotter, P.: Size distribution, mixing state and source apportionment of black carbon aerosol in London during wintertime, *Atmos. Chem. Phys.*, 14, 10061–10084, <https://doi.org/10.5194/acp-14-10061-2014>, 2014.
- Liu, J. W., Mo, Y. Z., Li, J., Liu, D., Shen, C. D., Ding, P., Jiang, H. Y., Cheng, Z. N., Zhang, X. J., Tian, C. G., Chen, Y. J., and Zhang, G.: Radiocarbon-derived source apportionment of fine carbonaceous aerosols before, during, and after the 2014 Asia-Pacific Economic Cooperation (APEC) summit in Beijing, China, *J. Geophys. Res.-Atmos.*, 121, 4177–4187, 2016.
- Menon, S., Hansen, J., Nazarenko, L., and Luo, Y. F.: Climate effects of black carbon aerosols in China and India, *Science*, 297, 2250–2253, 2002.
- Moteki, N. and Kondo, Y.: Effects of mixing state on black carbon measurements by laser-induced incandescence, *Aerosol Sci. Technol.*, 41, 398–417, 2007.
- Moteki, N. and Kondo, Y.: Method to measure time-dependent scattering cross sections of particles evaporating in a laser beam, *J. Aerosol Sci.*, 39, 348–364, 2008.
- Peng, J. F., Hu, M., Guo, S., Du, Z. F., Zheng, J., Shang, D. J., Zamora, M. L., Zeng, L. M., Shao, M., Wu, Y.-S., Zheng, J., Wang, Y., Glen, C. R., Collins, D. R., Molina, M. J., and Zhang, R. Y.: Markedly enhanced absorption and direct radiative forcing of black carbon under polluted urban environments, *P. Natl. Acad. Sci. USA*, 113, 4266–4271, 2016.
- Qin, Y. and Xie, S. D.: Spatial and temporal variation of anthropogenic black carbon emissions in China for the period 1980–2009, *Atmos. Chem. Phys.*, 12, 4825–4841, <https://doi.org/10.5194/acp-12-4825-2012>, 2012.
- Ramanathan, V. and Carmichael, G.: Global and regional climate changes due to black carbon, *Nat. Geosci.*, 1, 221–227, 2008.
- Ramanathan, V., Crutzen, P. J., Kiehl, J. T., and Rosenfeld, D.: Aerosols, climate, and the hydrological cycle, *Science*, 294, 2119–2125, 2001.
- Schnaiter, M., Linke, C., Möhler, O., Naumann, K. H., Saathoff, H., Wagner, R., Schurath, U., and Wehner, B.: Absorption amplification of black carbon internally mixed with secondary organic aerosol, *J. Geophys. Res.*, 110, D19204, <https://doi.org/10.1029/2005JD006046>, 2005.
- Schwarz, J. P., Gao, R. S., Fahey, D. W., Thomson, D. S., Watts, L. A., Wilson, J. C., Reeves, J. M., Darbeheshti, M., Baumgardner, D. G., Kok, G. L., Chung, S. H., Schulz, M., Hendricks, J., Lauer, A., Kärcher, B., Slowik, J. G., Rosenlof, K. H., Thompson, T. L., Langford, A. Q., Loewenstein, M., and Aikin, K. C.: Single-particle measurements of midlatitude black carbon and light-scattering aerosols from the boundary layer to the lower stratosphere, *J. Geophys. Res.*, 111, D16207, <https://doi.org/10.1029/2006JD007076>, 2006.
- Schwarz, J. P., Gao, R. S., Spackman, J. R., Watts, L. A., Thomson, D. S., Fahey, D. W., Ryerson, T. B., Peischl, J., Holloway, J. S., Trainer, M., Frost, G. J., Baynard, T., Lack, D. A., de Gouw, J. A., Warneke, C., and Del Negro, L. A.: Measurement of the mixing state, mass, and optical size of individual black carbon particles in urban and biomass burning emissions, *Geophys. Res. Lett.*, 35, L13810, <https://doi.org/10.1029/2008GL033968>, 2008.
- Schwarz, J. P., Gao, R. S., Perring, A. E., Spackman, J. R., and Fahey, D. W.: Black carbon aerosol size in snow, *Sci. Rep.*, 3, 1356, <https://doi.org/10.1038/srep01356>, 2013.
- Shiraiwa, M., Kondo, Y., Moteki, N., Takegawa, N., Miyazaki, Y., and Blake, D. R.: Evolution of mixing state of black carbon in polluted air from Tokyo, *Geophys. Res. Lett.*, 34, L16803, <https://doi.org/10.1029/2007GL029819>, 2007.
- Shiraiwa, M., Kondo, Y., Iwamoto, T., and Kita, K.: Amplification of light absorption of black carbon by organic coating, *Aerosol Sci. Technol.*, 44, 46–54, 2010.
- Song, S., Wu, Y., Xu, J., Ohara, T., Hasegawa, S., Li, J., Yang, L., and Hao, J.: Black carbon at a roadside site in Beijing: Temporal variations and relationships with carbon monoxide and particle number size distribution, *Atmos. Environ.*, 77, 213–221, 2013.
- Stephens, M., Turner, N., and Sandberg, J.: Particle identification by laser-induced incandescence in a solid-state laser cavity, *Appl. Optics*, 42, 3726–3736, 2003.
- Sun, Y. L., Jiang, Q., Wang, Z. F., Fu, P. Q., Li, J., Yang, T., and Yin, Y.: Investigation of the sources and evolution processes of severe haze pollution in Beijing in January 2013, *J. Geophys. Res.-Atmos.*, 119, 4380–4398, 2014.
- Wang, Q. Y., Huang, R. J., Cao, J. J., Han, Y. M., Wang, G. H., Li, G. H., Wang, Y. C., Dai, W. T., Zhang, R. J., and Zhou, Y. Q.: Mixing state of black carbon aerosol in a heavily polluted urban area of China: implications for light absorption enhancement, *Aerosol Sci. Technol.*, 48, 689–697, 2014a.
- Wang, Q. Y., Schwarz, J. P., Cao, J. J., Gao, R. S., Fahey, D. W., Hu, T. F., Huang, R. J., Han, Y. M., and Shen, Z. X.: Black carbon aerosol characterization in a remote area of Qinghai–Tibetan Plateau, western China, *Sci. Total Environ.*, 479–480, 151–158, 2014b.
- Wang, Q. Y., Huang, R.-J., Cao, J. J., Tie, X. X., Ni, H. Y., Zhou, Y. Q., Han, Y. M., Hu, T. F., Zhu, C. S., Feng, T., Li, N., and Li, J. D.: Black carbon aerosol in winter northeastern Qinghai–Tibetan Plateau, China: the source, mixing state and optical property, *Atmos. Chem. Phys.*, 15, 13059–13069, <https://doi.org/10.5194/acp-15-13059-2015>, 2015a.
- Wang, Q. Y., Liu, S. X., Zhou, Y. Q., Cao, J. J., Han, Y. M., Ni, H. Y., Zhang, N. N., and Huang, R. J.: Characteristics of Black

- Carbon Aerosol during the Chinese Lunar Year and Weekdays in Xi'an, China, *Atmosphere*, 6, 195–208, 2015b.
- Wang, Q. Y., Huang, R. J., Zhao, Z. Z., Cao, J. J., Ni, H. Y., Tie, X. X., Zhao, S. Y., Su, X. L., Han, Y. M., Shen, Z. X., Wang, Y. C., Zhang, N. N., Zhou, Y. Q., and Corbin, J. C.: Physicochemical characteristics of black carbon aerosol and its radiative impact in a polluted urban area of China, *J. Geophys. Res.-Atmos.*, 121, 12505–12519, <https://doi.org/10.1002/2016JD024748>, 2016.
- Wang, Y., Khalizov, A., Levy, M., and Zhang, R. Y.: New direction: light absorbing aerosols and their atmospheric impacts, *Atmos. Environ.*, 81, 713–715, 2013.
- Wang, Y. Q., Zhang, X. Y., and Arimoto, R.: The contribution from distant dust sources to the atmospheric particulate matter loadings at Xi'an, China during spring, *Sci. Total Environ.*, 368, 875–883, 2006.
- Wang, Y. Q., Zhang, X. Y., and Draxler, R. R.: TrajStat: GIS-based software that uses various trajectory statistical analysis methods to identify potential sources from long-term air pollution measurement data, *Environ. Modell. Softw.*, 24, 938–939, 2009.
- Wu, Y. F., Zhang, R. J., Tian, P., Tao, J., Hsu, S.-C., Yan, P., Wang, Q. Y., Cao, J. J., Zhang, X. L., and Xia, X. A.: Effect of ambient humidity on the light absorption amplification of black carbon in Beijing during January 2013, *Atmos. Environ.*, 124, 217–223, 2016.
- Yin, Z. and Wang, H.: Seasonal prediction of winter haze days in the north central North China Plain, *Atmos. Chem. Phys.*, 16, 14843–14852, <https://doi.org/10.5194/acp-16-14843-2016>, 2016.
- Yu, H. and Yu, J. Z.: Modal characteristics of elemental and organic carbon in an urban location in Guangzhou, China, *Aerosol Sci. Technol.*, 43, 1108–1118, 2009.
- Yu, H., Wu, C., Wu, D., and Yu, J. Z.: Size distributions of elemental carbon and its contribution to light extinction in urban and rural locations in the pearl river delta region, China, *Atmos. Chem. Phys.*, 10, 5107–5119, <https://doi.org/10.5194/acp-10-5107-2010>, 2010.
- Zhang, Q., Quan, J. N., Tie, X. X., Li, X., Liu, Q., Gao, Y., and Zhao, D. L.: Effects of meteorology and secondary particle formation on visibility during heavy haze events in Beijing, China, *Sci. Total Environ.*, 502, 578–584, 2015.
- Zhang, R., Jing, J., Tao, J., Hsu, S.-C., Wang, G., Cao, J., Lee, C. S. L., Zhu, L., Chen, Z., Zhao, Y., and Shen, Z.: Chemical characterization and source apportionment of PM<sub>2.5</sub> in Beijing: seasonal perspective, *Atmos. Chem. Phys.*, 13, 7053–7074, <https://doi.org/10.5194/acp-13-7053-2013>, 2013.
- Zhang, R. Y., Khalizov, A. F., Pagels, J. Zhang, D., Xue, H. X., and McMurry, P. H.: Variability in morphology, hygroscopicity, and optical properties of soot aerosols during atmospheric processing, *P. Natl. Acad. Sci. USA*, 105, 10291–10296, 2008a.
- Zhang, X. Y., Wang, Y. Q., Zhang, X., Guo, W., and Gong, S. L.: Carbonaceous aerosol composition over various regions of China during 2006, *J. Geophys. Res.*, 113, D14111, <https://doi.org/10.1029/2007JD009525>, 2008b.
- Zhang, Y.-L., Huang, R.-J., El Haddad, I., Ho, K.-F., Cao, J.-J., Han, Y., Zotter, P., Bozzetti, C., Daellenbach, K. R., Canonaco, F., Slowik, J. G., Salazar, G., Schwikowski, M., Schnelle-Kreis, J., Abbaszade, G., Zimmermann, R., Baltensperger, U., Prévôt, A. S. H., and Szidat, S.: Fossil vs. non-fossil sources of fine carbonaceous aerosols in four Chinese cities during the extreme winter haze episode of 2013, *Atmos. Chem. Phys.*, 15, 1299–1312, <https://doi.org/10.5194/acp-15-1299-2015>, 2015.
- Zheng, G. J., Duan, F. K., Su, H., Ma, Y. L., Cheng, Y., Zheng, B., Zhang, Q., Huang, T., Kimoto, T., Chang, D., Pöschl, U., Cheng, Y. F., and He, K. B.: Exploring the severe winter haze in Beijing: the impact of synoptic weather, regional transport and heterogeneous reactions, *Atmos. Chem. Phys.*, 15, 2969–2983, <https://doi.org/10.5194/acp-15-2969-2015>, 2015.